

# Glycation of soy and pea proteins influences infant gastric digestibility more than intestinal digestibility

Jiaying Tang<sup>a</sup>, Harry J. Wichers<sup>b,c</sup>, Kasper A. Hettinga<sup>a,\*</sup>

<sup>a</sup> Food Quality & Design Group, Wageningen University & Research, Wageningen, the Netherlands

<sup>b</sup> Wageningen Food & Biobased Research, Wageningen University & Research, Wageningen, the Netherlands

<sup>c</sup> Laboratory of Food Chemistry, Wageningen University and Research, Wageningen, the Netherlands

## ARTICLE INFO

### Keywords:

Soy protein  
Pea protein  
Dry heating  
Glycation  
Infant digestion  
Infant formula

## ABSTRACT

Dry heating of plant proteins occurs during production of plant-based infant formula. To study the effect of dry heating on physicochemical changes and *in vitro* infant digestion of soy and pea proteins, these proteins were mild dry heated (60 °C) for 6 h and 48 h, in the presence or absence of glucose. In this study, we found that with extended dry heating, the degrees of glycation increased in the presence of glucose. After 48 h of dry heating, the degree of gastric hydrolysis decreased from 2.7% to 0.2% for soy protein and from 2.8% to 0.4% for pea protein, compared to non-treated proteins. Such resistance to gastric digestion was probably due to the extensive protein aggregation induced by glycation. However, the intestinal digestion was less affected, as the degree of hydrolysis was similar at the end of intestinal digestion, ranging from 31.0% to 35.4% for soy protein and 36.7% to 48.5% for pea protein. This may be due to the broad range of proteases in pancreatin negating the effect of glycation. By contrast, for the glucose-free samples, no glycation happened and only limited insoluble aggregates were formed during dry heating. Despite this aggregation, the variation in dry heating duration did not lead to different digestibility. Therefore, 60 °C of mild dry heating will influence the gastric digestion of glucose-containing samples, but will not influence the final intestinal digestibility of all the samples with or without glucose.

## 1. Introduction

Proteins are a key factor in infant formulas (IFs) to provide sufficient essential amino acids (EAAs) to meet the needs for the growth and development of infants. In recent years, there is increasing interest to apply plant proteins, such as soy protein (SP), in IFs. SP-based IFs have been commercially available for decades. Apart from the sustainability consideration, an important objective is to alleviate cow's milk allergy (CMA). CMA occurs especially in infants because of their immature immune system. SP is the only legally accepted legume protein source in the European Union according to the [European Commission \(2016\)](#). However, SP can be an allergen for some infants. In addition, the trypsin inhibitors in SP, as one of the anti-nutritional factors, may limit the digestion and lower the bioavailability of EAAs ([Martín-Cabrejas et al., 2009](#)). Therefore, innovative legumes need to be explored as soy alternatives to develop plant-based IFs. Among all the legumes, pea protein (PP) is considered a promising alternative for SP. Compared to SP, PP still has a high PDCAAS (protein digestibility corrected amino acid score), as well as relatively lower allergenicity and fewer

anti-nutritional factors ([Gorissen et al., 2018](#); [Le Roux et al., 2020](#); [Rutherford, Fanning, Miller, & Moughan, 2014](#)).

Production of powdered IFs involves thermal processing such as spray drying, pasteurization, and sterilization, during which the Maillard reaction may occur. The Maillard reaction, also known as glycation, is a spontaneous and non-enzymatic reaction between amino groups of proteins/peptides/amino acids and reducing sugars. Especially lysine residues are sensitive to glycation. Glycation can be characterized into three stages: early, advanced, and final stages; these three stages can occur simultaneously ([de Oliveira, Coimbra, de Oliveira, Zuñiga, & Rojas, 2016](#)). During the early stage of glycation, lysine residues covalently react with reducing sugars and initially undergo irreversible rearrangement, to form Amadori products such as furosine (Nε-2-furoylmethyllysine). It is known that lysine is one of the limiting amino acids in the diet. Therefore, the lysine damage during this stage may limit its bioavailability and thereby reduce the overall nutritional value of proteins. The advanced stage involves the further reaction of Amadori products, resulting in the formation of various advanced glycation end products (AGEs), e.g., CML (Nε-carboxymethyllysine) and

\* Corresponding author.

E-mail address: [kasper.hettinga@wur.nl](mailto:kasper.hettinga@wur.nl) (K.A. Hettinga).

<https://doi.org/10.1016/j.foodhyd.2022.108251>

Received 3 June 2022; Received in revised form 25 September 2022; Accepted 18 October 2022

Available online 22 October 2022

0268-005X/© 2022 The Authors. Published by Elsevier Ltd. This is an open access article under the CC BY license (<http://creativecommons.org/licenses/by/4.0/>).

CEL (N $\epsilon$ -carboxyethyllysine). This is followed by the formation of brown nitrogenous polymers such as melanoidins at the final stage of glycation (Tamanna & Mahmood, 2015). The mechanism of this reaction remains unclear due to the occurrence of multiple complex chemical reactions. Moreover, glycation is affected by the nature of reactants, heating temperature and time, as well as water activity and pH (Kutzli, Weiss, & Gibis, 2021). It has also been reported that glycation is more intense when reactants are dry heated (i.e., in a powdered form), where the higher heating temperatures and longer heating durations can also increase the reaction rate (de Oliveira et al., 2016; Schong & Famelart, 2017).

During dry heating, next to glycation, also protein denaturation and aggregation normally happen. In general, the protein structural modifications by glycation and heating cannot be easily distinguished. In addition, such variation in protein structure may further influence protein digestion. Our previous study showed that the digestibility may increase when heat-induced protein unfolding partially denatures the protein, due to increased accessibility to digestive enzymes (Tang, Wichers, & Hettinga, 2022). However, aggregation and glycation may also bury the enzyme-cleavage sites, and thereby negatively affect digestion (Corzo-Martínez, Soria, Belloque, Villamiel, & Moreno, 2010; Wada & Lönnerdal, 2014). For instance, it is known that glycation mainly occurs at the lysine residues, which are the specific cleavage sites of trypsin as well (Hemmler et al., 2019; Olsen, Ong, & Mann, 2004). Therefore, when these sites are blocked by glycation, they cannot be recognized by trypsin, and this may thus have negative consequences for intestinal digestion.

Previous research mostly focused on the glycation modification of plant proteins, for the purpose of improving their techno-functional properties (Feng, Berton-Carabin, Atac Mogol, Schroen, & Fogliano, 2021; Kutzli et al., 2021; Zhao et al., 2022), whereas the effect of glycation on plant protein digestibility has been studied to a much smaller extent. Especially there is no research reported when it comes to *in vitro* infant digestion. Therefore, this study aimed at exploring the effect of glycation of SP and PP on protein structures, and their consequences for infant digestibility. To achieve this aim, we selected glucose as the reducing sugar, as glucose from corn syrup is the main reducing sugar in soy-based infant formulas. SP and PP were then dry-heated with glucose for different heating durations, to mimic different glycation levels in actual processing and storage conditions of infant formulas. Subsequently, the level of glycation and protein physicochemical changes were determined. Afterward, all the glycated proteins were subjected to a full-term infant digestion model system, and the level of digestion was measured.

## 2. Materials and methods

### 2.1. Materials and chemicals

Fresh soybean (Glycine max; protein content: 39.3%, w/w) was obtained from Wageningen Plant Research, Lelystad, the Netherlands (courtesy ing. Ruud Timmer), and pea (Pisum sativum L.; protein content: 23.3%, w/w) was purchased from a local retailer (Brand name: HAK). Protein concentration was determined through Bicinchoninic Acid (BCA) Protein Assay Kit or through DUMAS Flash EA 1112 Protein analyzer from Thermo Fisher Scientific (Massachusetts, USA). LDS sample buffer (4 $\times$ ), reducing agent (10 $\times$ ), 12% Bis-Tris gel, prestained protein ladder, and MOPS SDS running buffer were also obtained from Thermo Fisher Scientific (Massachusetts, USA). D-Glucose, porcine pepsin, and porcine pancreatin, as well as all other chemicals, were obtained from Sigma-Aldrich (Missouri, USA) unless otherwise stated.

### 2.2. Preparation of protein samples and dry heating

Soy protein (SP) and pea protein (PP) were isolated as described previously (Tang et al., 2022). Protein contents of powdered SP and PP

were 77.0% and 79.2%, respectively, according to DUMAS, with a nitrogen-to-protein conversion factor of 5.7. SP and PP powders were dry-heated in an incubator at 60 °C for 0 h (T0, i.e., non-treated control), 6 h (T6), or 48 h (T48) in the presence of glucose (SP-G and PP-G). The protein-to-glucose weight ratio was set to be 1:4, as this ratio is normal in IFs. The control groups were treated the same, but without added glucose (SP and PP). The relative humidity was controlled at 60% through a desiccator with a saturated potassium iodide solution. Heat treatment was performed in independent duplicates. All the samples were stored at -20 °C until use.

### 2.3. Color measurement

The color of the dry-heated samples was measured in duplicate by using a ColorFlex CX2189 Spectrophotometer (HunterLab, Virginia, USA). The color value was expressed by three chromaticity coordinates: L\* (lightness), a\* (redness), and b\* (yellowness). Browning index (BI), as an important parameter in glycation, was calculated by equations (1) and (2) according to Consoli et al. (2018):

$$BI = \frac{x - 0.31}{0.172} \times 100 \quad (1)$$

$$x = \frac{(a^* + 1.75L^*)}{(5.645L^* + a^* - 3.012b^*)} \quad (2)$$

### 2.4. Sodium dodecyl sulfate-polyacrylamide gel electrophoresis (SDS-PAGE)

Reducing SDS-PAGE was performed to analyze protein composition and the disappearance of intact protein after digestion. Prior to analysis, all the samples were centrifuged to remove the insoluble parts. The supernatants were mixed with LDS sample buffer (4 $\times$ ) and reducing agent (10 $\times$ ), and then diluted with ultrapure water. These sample mixtures were incubated at 70 °C for 10 min in a heating block. Undigested samples containing ~15  $\mu$ g protein or digested samples containing ~10  $\mu$ g protein were loaded onto a 12% Bis-Tris gel. A prestained protein ladder (10–140 kDa) was used as molecular weight marker. Gels were run under constant 120 V for 90 min with MOPS SDS running buffer. Gels were stained by Coomassie brilliant blue R-250 (Bio-Rad, California, USA) and destained by washing buffer (7.5% acetic acid, 10% ethanol).

### 2.5. Analysis of glycation markers by LC-MS/MS

Quantification of glycation markers—lysine, furosine (N $\epsilon$ -2-furoylmethyllysine) and CML (N $\epsilon$ -carboxymethyllysine) of non-treated and dry-heated samples was conducted on a high-performance liquid chromatograph coupled to a triple quadrupole mass spectrometer (LC-MS/MS, series: LCMS-8050, Shimadzu Corporation, Kyoto, Japan), according to the methods of Troise, Fiore, Roviello, Monti, and Fogliano (2015) and Zenker et al. (2019) with some modifications. Briefly, sample powders containing 2.5 mg protein (based on DUMAS results) were mixed with 4 mL 6 M HCl and heated at 110 °C for 22 h in a heating block for acid hydrolysis. Nitrogen was saturated in the heating tubes to avoid interference from oxidation. After acid hydrolysis, the hydrolysates were dried under nitrogen and reconstituted in 4 mL ultrapure water, followed by filtration (0.22  $\mu$ m filter) and centrifugation (10,000 $\times$ g, 10 min, 20 °C) to remove insoluble parts. Subsequently, 20  $\mu$ L of the filtered supernatants were mixed with 180  $\mu$ L 50% (v/v) acetonitrile and 10  $\mu$ L internal standard. The internal standard was 10 ppm of mixed d4-lysine, d4-furosine and d2-CML. Calibration standards were 200  $\mu$ L 0–10 ppm of mixed lysine, furosine, and CML, spiked with 10  $\mu$ L internal standard. For analysis, 5  $\mu$ L of each sample was injected into the LC-MS/MS system and measured in duplicate. Calibration curves were linearly regressed as peak area ratio of standards/internal standard

against corresponding standards' concentration. Lysine, furosine, and CML were quantified according to the calibration curves and their peak area ratio (analytes/internal standards). The final content was shown as mg/g protein for lysine and furosine, as well as mg/100 g protein for CML.

## 2.6. Particle size distribution (PSD)

PSD was determined for two fractions: the full suspension and the supernatant. The suspension was measured by laser diffraction by Mastersizer 3000 (Malvern Instruments, Worcestershire, UK); whereas the supernatant was measured by dynamic light scattering by Zetasizer Ultra (Malvern Instruments, Worcestershire, UK) (Feng et al., 2021). The refractive indexes of both systems were set to be 1.45 and 1.33 for the dispersed phase and continuous phase, respectively. Briefly, sample powders containing 0.25 g protein were dissolved in 5 mL 10 mM PBS buffer (pH 7.4) and divided into two portions. One portion of the suspensions was gradually dropped into the analyst chamber of the Mastersizer system until the obscuration rate was between 10 and 20%, after which the PSD was measured in triplicate. Another portion was centrifuged (10,000×g, 10 min, 20 °C) and filtrated with a 0.45 μm filter. The supernatants were diluted to 1 mg/mL according to DUMAS results. About 1 mL of the sample solutions were transferred into the Zetasizer system and measured in triplicate. All the results were shown as volume-weighted PSD.

## 2.7. Surface hydrophobicity

The 8-anilino-1-naphthalenesulfonic acid ammonium salt (ANSA) fluorescence assay was performed to measure the surface hydrophobicity of soluble proteins, as previously described (Tang et al., 2022). Briefly, samples were dissolved in 10 mM PBS buffer (pH 7.4) and centrifuged. All the supernatants were diluted to 0.15 mg/mL. Subsequently, 25 μL of the supernatants were mixed with 200 μL 0.8 mM ANSA reagent (prepared in 10 mM PBS buffer, pH 7.4) in a 96-well black polystyrene plate. After incubation in the dark for 10 min, the fluorescence intensity was measured in duplicate at 390 nm (excitation) and 470 nm (emission) by Infinite® 200 PRO NanoQuant with i-control software (Tecan, Männedorf, Switzerland). PBS buffer with ANSA was set as blank. Results were displayed as fluorescence intensity corrected for protein concentration (based on BCA results) and blank.

## 2.8. In vitro static infant gastrointestinal digestion

Infant *in vitro* digestion was performed with a full-term infant digestion model according to Ménard et al. (2018). All the sample powders were dispersed in 10 mM PBS buffer (pH 7.4), and their protein concentrations were adjusted to 12 mg/mL to mimic infant formula. For the gastric phase (GP), digestion was conducted for 60 min at 37 °C with 268 U/mL pepsin at pH 5.3 and stopped by increasing the pH to 6.6. For the intestinal phase (IP), digestion was conducted for 60 min at 37 °C with 16 U/mL trypsin in pancreatin at pH 6.6 and stopped by adding 5 mM Pefabloc. Sampling points were G0 (0 min, before digestion), G10 and G60 (10 min and 60 min of the GP), as well as I10 and I60 (10 min and 60 min of the IP). Digestions were independently performed in duplicate. All the samples were stored at −20 °C for later use.

## 2.9. Degree of hydrolysis

Degree of hydrolysis (DH) after digestion was determined by o-phthalaldehyde (OPA) assay according to Mulet-Cabero, Rigby, Brodkorb, and Mackie (2017) with some modifications. Briefly, GP and 3-fold diluted IP samples were mixed with 10% cooled trichloroacetic acid (TCA, w/v) in a volume ratio of 5:4 and then centrifuged at 10,000×g for 30 min. Afterward, 10 μL of all the TCA-containing supernatants were added to a 96-well transparent polystyrene plate with 200

μL OPA working reagent. The plate was incubated for 15 min in the dark, and the absorbance was measured in duplicate at 340 nm by Infinite® 200 PRO NanoQuant with i-control software (Tecan, Männedorf, Switzerland). The calibration curve was made by using 0–10 mM L-leucine. The DH was calculated by the following equation (3):

$$DH(\%) = \frac{NH_2(\text{final}) - NH_2(\text{initial})}{NH_2(\text{acid}) - NH_2(\text{initial})} \times 100 \quad (3)$$

where NH<sub>2</sub>(final) refers to the concentration of free amino groups at different sampling points, NH<sub>2</sub>(initial) refers to the concentration of free amino groups before digestion (G0), and NH<sub>2</sub>(acid) refers to the concentration of the total free amino groups after acid hydrolysis (6 M HCl, 110 °C, 24 h).

## 2.10. Quantification of nitrogen transfer after in vitro digestion

Nitrogen transfer represented the total soluble nitrogen transfer from the insoluble sample material to the digestive fluids during digestion. The soluble nitrogen contents of samples at G0, G60, and I60 were measured by DUMAS, according to Zenker, Raupbach, Boeren, Wichers, and Hettinga (2020). The percentage of nitrogen transfer was calculated as the soluble nitrogen content of the digesta relative to the theoretical maximum nitrogen content (i.e., assuming 12 mg/mL of proteins were completely dissolved). The nitrogen contents in enzyme controls were subtracted to compensate for the extra introduction of nitrogen. Enzyme controls were the same as other digestion samples, but the protein samples were replaced by ultrapure water. All samples were analyzed from duplicate digestions in technical duplicate.

## 2.11. Statistical analysis

All the data were visualized by GraphPad Prism 9.0 software and analyzed through IBM SPSS 25.0 software by one-way ANOVA with Duncan post-hoc test. Differences were considered significant when  $p < 0.05$ .

# 3. Results and discussion

## 3.1. Level of glycation

### 3.1.1. Quantification of glycation markers by LC-MS/MS

Lysine, furosine, and CML are regarded as glycation markers, reflecting the different glycation levels. Lysine residues react with reducing sugars during dry heating, forming furosine at the early stage and CML at the advanced stage of glycation.

Regarding the glucose-free systems (SP and PP), no obvious glycation happened upon dry heating in the absence of reducing sugar (Fig. 1), as expected. Almost no significant differences ( $p > 0.05$ ) were found in the contents of lysine, furosine and CML among the different heating durations (T0, T6, and T48).

For the glucose-containing systems (SP-G and PP-G), as shown in Fig. 1A, the lysine contents were 100.0 mg/g protein and 114.4 mg/g protein at T0 for samples of SP-G and PP-G, respectively. After dry heating for 6 h (T6) to 48 h (T48), the lysine content of both SP-G and PP-G decreased, by approximately 25% at T6 and 57% at T48 for SP-G, as well as by 23% and 57% for PP-G, compared to T0, with these decreases being significant ( $p < 0.05$ ). These results suggest that glycation was aggravated in SP-G and PP-G systems after dry heating from 6 h to 48 h. Furosine contents can be seen in Fig. 1B. The starting furosine contents were 1.4 mg/g protein in SP-G and SP samples and 1.3 mg/g protein in PP-G and PP samples. At T6, for SP-G and PP-G the furosine level was about 16 times higher than at T0, reaching approximately 22 mg/g protein; from T6 to T48, the furosine contents further increased by ~58% in SP-G and by ~60% in PP-G. This sharp increase in furosine in the first 6 h was due to the active Amadori rearrangement happening at

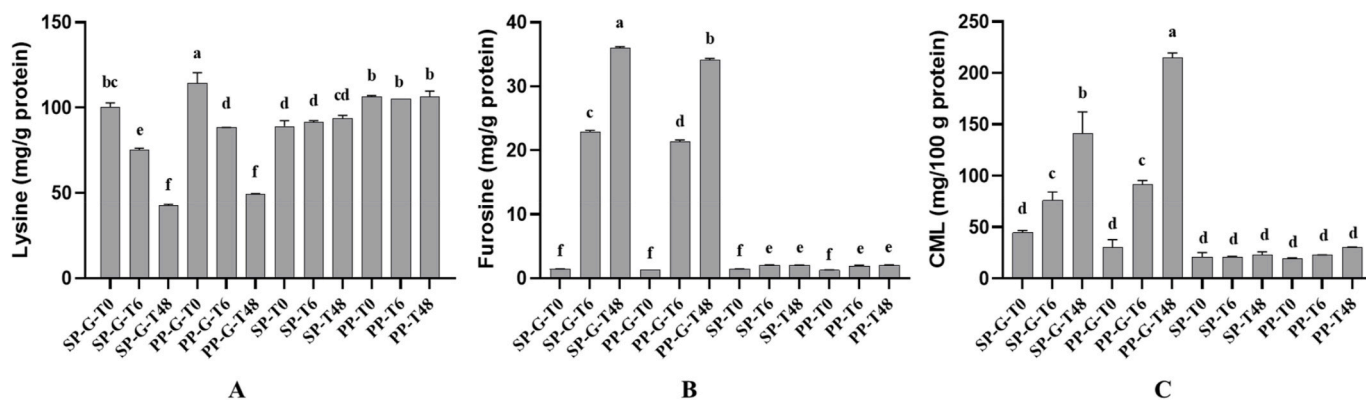


Fig. 1. Contents of glycation markers (A) lysine, (B) furosine, and (C) CML of SP-G, PP-G, SP and PP upon different heating durations, as measured by LC-MS/MS. Error bars represent standard deviations of duplicates. Statistical differences were analyzed with ANOVA and Duncan post-hoc test. Different letters above the bars represent significant differences ( $p < 0.05$ ).

the early stage of glycation. As displayed in Fig. 1C, for the T0 samples, the CML contents were 44.7 mg/100 g protein in SP-G and 30.5 mg/100 g protein in PP-G. For SP-G, the contents of CML at T6 and T48 were ~2 and 3 fold higher than at T0, respectively. For PP-G, the contents of CML at T6 and T48 were ~3 and 7 times higher than at T0, respectively. This suggests that glycation for PP-G was more advanced than for SP-G. To the best of our knowledge, there have not been other studies simultaneously comparing the CML contents of SP-G and PP-G.

3.1.2. Color

The browning index (BI) was used to monitor color development and obtain information on final stage glycation levels. In Table 1, for the glucose-containing samples, the increase in BI was approximately 41% in SP-G and 23% in PP-G from T0 to T6, whereas at T48, the BI was ~6 and ~5 times higher than at T0 for SP-G and PP-G, respectively. Thus, dry heating of SP-G and PP-G for 48 h, as expected, showed a much larger extent of the final stage of glycation than dry heating for 6 h. In addition, for glucose-free samples, the increase in BI was slower. However, it was noticed that from T6 to T48, BI increased by around 42% in SP while only by around 12% in PP. The color development of SP was thus more obvious than of PP at T48, although no significant formation of CML was found (Fig. 1C). Therefore, the BI increase in SP was not attributed to glycation but may be due to the browning of flavonoids during dry heating (Muliterno, Rodrigues, de Lima, Ida, & Kurozawa, 2017). First, soybean has a higher total flavonoid content than pea seed (Xu, Yuan, & Chang, 2007). Second, during acid extraction of proteins, the hydrophobic association between proteins and flavonoids led to their co-precipitation (Charlton et al., 2002; Li et al., 2014). Taken together, we speculate that SP will have a relatively higher amount of flavonoids than PP, which may result in non-glycation browning after 48 h of dry heating.

Table 1

Color values ( $L^*$  = lightness,  $a^*$  = redness, and  $b^*$  = yellowness) and browning index (BI) of powdered SP-G, PP-G, SP and PP upon different heating durations. Statistical differences were analyzed with ANOVA and Duncan post-hoc test. Different letters within different index columns represent significant differences ( $p < 0.05$ ).

	T0				T6				T48			
	$L^*$	$a^*$	$b^*$	BI	$L^*$	$a^*$	$b^*$	BI	$L^*$	$a^*$	$b^*$	BI
SP-G	89.54 ± 0.01 <sup>a</sup>	-0.65 ± 0.01 <sup>h</sup>	6.17 ± 0.10 <sup>l</sup>	6.36 ± 0.11 <sup>j</sup>	88.81 ± 0.01 <sup>b</sup>	-0.77 ± 0.01 <sup>i</sup>	8.42 ± 0.11 <sup>j</sup>	8.97 ± 0.13 <sup>i</sup>	76.93 ± 0.09 <sup>f</sup>	3.58 ± 0.09 <sup>b</sup>	24.69 ± 0.14 <sup>a</sup>	40.82 ± 0.27 <sup>a</sup>
PP-G	89.04 ± 0.16 <sup>b</sup>	-0.49 ± 0.01 <sup>g</sup>	7.87 ± 0.02 <sup>k</sup>	8.52 ± 0.02 <sup>i</sup>	88.12 ± 0.02 <sup>c</sup>	-0.52 ± 0.02 <sup>g</sup>	9.44 ± 0.01 <sup>i</sup>	10.50 ± 0.02 <sup>h</sup>	74.04 ± 0.33 <sup>e</sup>	4.05 ± 0.05 <sup>a</sup>	23.38 ± 0.03 <sup>b</sup>	40.73 ± 0.32 <sup>a</sup>
SP	85.13 ± 0.16 <sup>d</sup>	-0.50 ± 0.01 <sup>g</sup>	11.11 ± 0.07 <sup>h</sup>	13.06 ± 0.05 <sup>g</sup>	85.55 ± 0.16 <sup>d</sup>	-0.37 ± 0.01 <sup>f</sup>	12.20 ± 0.04 <sup>g</sup>	14.52 ± 0.10 <sup>f</sup>	85.26 ± 0.01 <sup>d</sup>	0.34 ± 0.01 <sup>d</sup>	16.19 ± 0.04 <sup>c</sup>	20.62 ± 0.07 <sup>b</sup>
PP	83.57 ± 0.18 <sup>e</sup>	-0.07 ± 0.02 <sup>c</sup>	13.40 ± 0.11 <sup>f</sup>	16.80 ± 0.12 <sup>e</sup>	84.08 ± 0.26 <sup>e</sup>	-0.09 ± 0.01 <sup>e</sup>	14.09 ± 0.23 <sup>e</sup>	17.62 ± 0.25 <sup>d</sup>	83.74 ± 0.14 <sup>e</sup>	0.64 ± 0.04 <sup>c</sup>	15.13 ± 0.23 <sup>d</sup>	19.80 ± 0.33 <sup>c</sup>

3.2. Physicochemical changes

3.2.1. Protein composition

The reducing SDS-PAGE results represent the subunit composition of soluble soy and pea proteins with/without glucose after dry heating (Fig. 2). Native SP and PP were mainly composed of globular proteins, namely  $\beta$ -conglycinin (7S) and glycinin (11S) for SP, and vicilin (7S), convicilin (7-8S), and legumin (11S) for PP, which was in line with our previous study (Tang et al., 2022).

For glucose-free SP and PP, the subunit composition remained almost unchanged when dry heated from 6 h to 48 h, compared to samples at T0. For glucose-containing SP-G and PP-G, glycation became more intense when dry heating lasted 48 h, as represented by the subunits shifting up and some of them becoming lighter or even disappearing, which is consistent with a previous study by Fu et al. (2021). The shifting up of subunits was due to glucose being attached to proteins by covalent reactions during glycation, hence the increase in molecular weights. Moreover, the decrease and disappearance of the subunits were very clear in the samples with glucose at T48. The reason is that, at the advanced and final stages of glycation, crosslinking and aggregation occurred among glycated proteins, leading to larger aggregates being formed (Wang, Yuan, Zhou, & Gu, 2021). Those aggregates would mostly be left in the precipitate after centrifugation of the samples, thus not being visible on the gels.

3.2.2. Particle size distribution

The PSD of both suspension and supernatant after dry heating is shown in Fig. 3. For the suspensions in general (Fig. 3 A&B), the particle sizes of proteins heated with glucose were larger than those without glucose. Moreover, as the heating time increased, the small-sized fractions decreased, while the large-sized fractions increased simultaneously. The particle sizes were mostly in the range of 10–100  $\mu$ m. Only

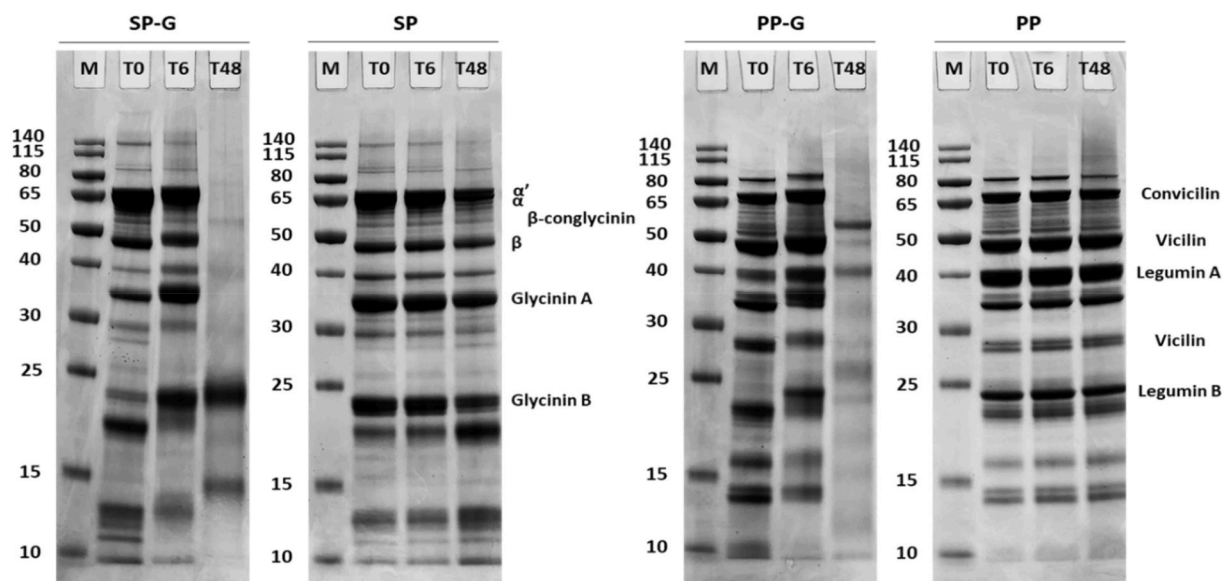


Fig. 2. Protein composition of soluble SP-G, SP, PP-G and PP upon different heating durations. Lane M: molecular weight marker from 10 to 140 kDa.

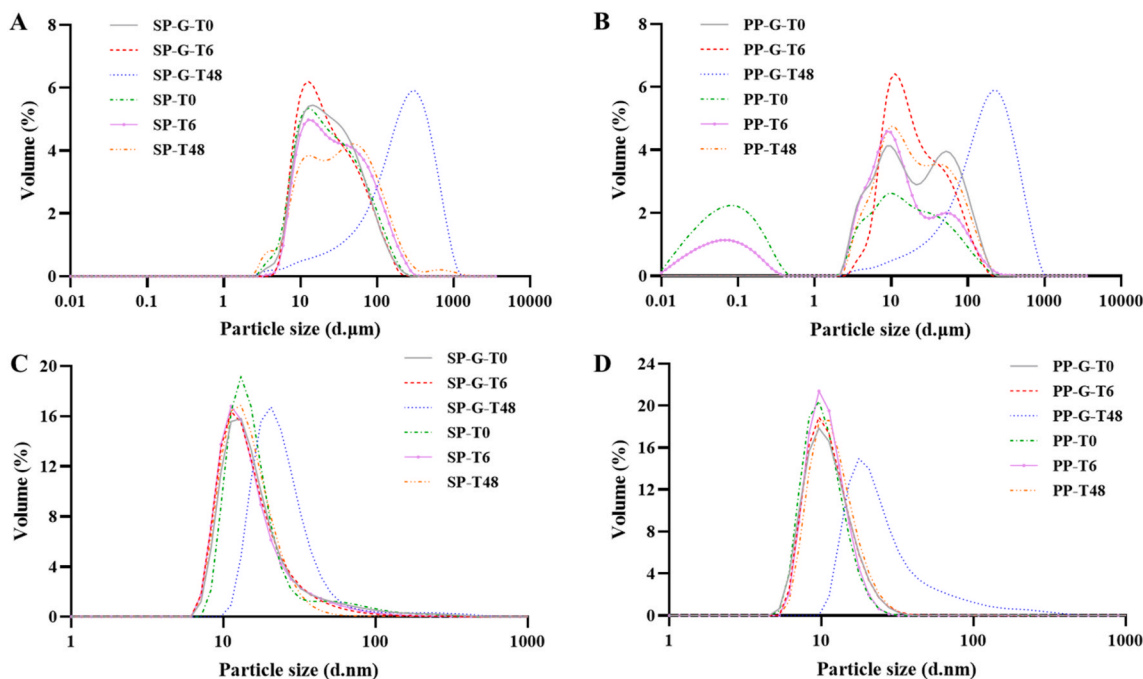


Fig. 3. Particle size distribution for suspension (A) & (B) and supernatant (C) & (D) of SP-G, PP-G, SP and PP upon different heating durations, respectively. Results were shown as volume-weighted particle size distribution.

the samples of SP-G-T48 and PP-G-T48 had extremely large particles, the sizes of which were mostly centered at around 310  $\mu\text{m}$  and 220  $\mu\text{m}$ , respectively. These results indicate that dry heating did enhance protein aggregation, but glycation that happened in the glucose-containing samples contributed much more to the overall level of aggregation.

For the supernatants containing only the soluble proteins (Fig. 3 C&D), the PSD curves almost overlapped. The most frequently occurring sizes were around 12 nm for SP-G and SP, as well as around 10 nm for PP-G and PP, as these numbers were the sizes of the monodispersed protein molecules. However, strong aggregation was observed in the samples of SP-G-T48 and PP-G-T48, similar to the suspensions. This is because larger soluble aggregates formed, which was further confirmed by the surface hydrophobicity data at T48 (see section 3.2.3).

Regarding the mechanisms of aggregation, for the glucose-free systems, the formation of large particles may be due to heat-induced aggregation. According to [Kavanagh, Clark, and Ross-Murphy \(2000\)](#) and [Li et al. \(2007\)](#), globular proteins first form oligomers by heat-induced disulfide rearrangement and subsequently form aggregates by non-covalent forces (e.g., hydrogen bonds and hydrophobic interactions). For the glucose-containing systems, it is estimated that proteins and glucose were first covalently conjugated during glycation, and then the conjugates were further aggregated mainly by hydrophobic-hydrophobic interactions ([Wang et al., 2021](#)). For SP-G-T48 and PP-G-T48, the reason why soluble aggregates formed was likely to be that the net charges on the surface and repulsive forces kept them soluble ([Spotti et al., 2019](#)).

### 3.2.3. Surface hydrophobicity

Surface hydrophobicity is an indicator for the distribution of hydrophobic amino acid residues on the protein surface. The surface hydrophobicity of soluble proteins was shown in Fig. 4. Generally, glucose-containing proteins had lower surface hydrophobicity than glucose-free proteins, due to glucose being covalently bound with lysine residues and forming hydrophilic glycation products on the protein surface after dry heating. In SP-G and PP-G, the surface hydrophobicity at T48 was about 13 and 6 times lower than that at T0, respectively, which could be attributed to the highest level of glycation at T48. Furthermore, the surface hydrophobicity in SP and PP remained stable after heating, except that SP-T48 showed a significant decline by approximately 43% in the surface hydrophobicity ( $p < 0.05$ ), compared to SP-T0. One possible reason may be that the long-time dry heating (T48) led to the hydrophobic binding between SP and flavonoids, thereby decreasing the fluorescence intensity, as previously shown by [Yuksel, Avci, and Erdem \(2010\)](#). Thus, this decline is unlikely to represent that the tertiary structure of SP was affected.

### 3.3. In vitro protein digestion of dry-heated samples

#### 3.3.1. Degree of hydrolysis

The degree of hydrolysis (DH) after digestion were shown in Fig. 5. Generally, the phenomenon that glycation limited the DH was obvious in gastric digestion, and the overall DH of glucose-containing samples after intestinal digestion was relatively lower compared to glucose-free samples. Moreover, SP had a relatively lower DH than PP, whether in the presence or absence of glucose.

In the GP, the DH of all the samples ranged from 0.2% to 2.8%. The reason for the low gastric DH was the relatively high pH of 5.3, and the low pepsin activity of 268 U/mL, reflecting infant digestion conditions. Both SP-G and PP-G showed a similar declining trend in the DH with extended dry heating, with significant differences between T6 and T48 ( $p < 0.05$ ). As digestion progressed from G10 to G60, the DH increased significantly ( $p < 0.05$ ) for the samples at T0 and T6, whereas that at T48 remained unchanged ( $p > 0.05$ ). At the end of gastric digestion (G60), the DH was only 0.2% and 0.4% for SP-G-T48 and PP-G-T48, respectively. These results indicate that highly glycated proteins have a strong resistance to gastric digestion. This was due to the glycation-induced aggregation, which will be further explained later in section 3.4. For SP and PP, no significant differences in the DH were found after different heating durations ( $p > 0.05$ ), whereas the differences from G10 to G60 were significant ( $p < 0.05$ ). Therefore, different heating intensities would not influence the gastric digestibility of these proteins in the absence of reducing sugars, being in line with previously published research ([Rivera del Rio et al., 2020](#)).

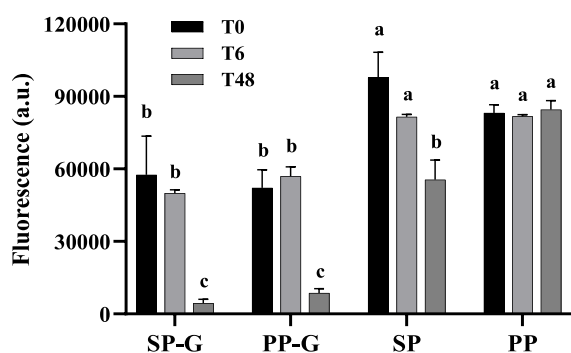


Fig. 4. Surface hydrophobicity of soluble SP-G, PP-G, SP and PP upon different heating durations. Error bars represent standard deviations of duplicates. Statistical differences were analyzed with ANOVA and Duncan post-hoc test. Different letters above the bars represent significant differences ( $p < 0.05$ ).

The DH in the IP was much higher than in the GP, as the intestinal digestion was conducted at pH 6.6, near the optimal pH of the enzymes in pancreatin. The values of the DH among all the samples in the IP were between 28.2% and 62.3%. From T0 to T48, the DH of both SP-G and PP-G tended to decrease. However, this trend was not significant in SP-G ( $p > 0.05$ ), but significant only from T6 to T48 in PP-G ( $p < 0.05$ ). This indicates that PP-G was more sensitive to dry heating than SP-G, which was also confirmed by its relatively higher CML levels (Fig. 1C), indicating that especially the advanced stage of glycation reduces the digestibility of proteins. Regarding SP and PP, the results in the IP were all the same ( $p > 0.05$ ) after different heating durations. This suggests that the effect of different dry heating times of full suspensions (without reducing sugars) on intestinal digestion was negligible, similar to gastric digestion. In addition, from I10 to I60, SP and PP increased about 20% in the DH ( $p < 0.05$ ). But interestingly, for SP-G and PP-G, this increasing trend was not significant ( $p > 0.05$ ), with their DH increasing no more than ~6%. Therefore, at the end of intestinal digestion, samples with glucose had a relatively lower overall DH than those without glucose, independent of heating time.

Comparing the protein sources, the overall DH (I60) of PP was higher than that of SP. Likewise, the overall DH of PP-G was higher than that of SP-G. This is probably because SP contains more trypsin inhibitors than PP, and 60 °C of mild dry heating as applied here will not have fully inactivated these trypsin inhibitors, leading to the lower DH in SP and SP-G ([Gilani, Cockell, & Sepehr, 2019](#); [Stewart, Raghavan, Orsat, & Golden, 2003](#)).

#### 3.3.2. Nitrogen transfer

Nitrogen transfer during digestion was determined by monitoring the nitrogen solubilization in the digestive fluids (Fig. 6). Before digestion (G0), the percentage of soluble nitrogen in the supernatants was representative of the protein solubility to some extent. For all the samples, the solubility was around 50% for T0; but decreased to only 7.2% (SP-G and PP-G), 33.5% (SP), and 21.4% (PP) for T48. This decrease in solubility reflects the formation of aggregates, as confirmed by the PSD results (Fig. 3). For those T48 samples, the initial content of soluble nitrogen (at G0) was the lowest among all samples. During digestion, the increase in the nitrogen transfer of SP-G and SP was not significant between G0 and G60 ( $p > 0.05$ ), but significant between G60 and I60 ( $p < 0.05$ ). In comparison, for PP-G and PP, the increasing trend in nitrogen transfer was significant ( $p < 0.05$ ) between all different digestion stages (G0, G60, and I60).

In addition, at the end of digestion (I60), all the samples reached their highest level of soluble nitrogen, being similar among all samples, except for SP-G-T48 and PP-G-T48 with relatively lower levels. However, despite so, these similar levels of nitrogen transfer did not translate to similar DH levels at I60. As discussed earlier, SP and PP had a higher overall DH (I60) than SP-G and PP-G. Therefore, the absence of a correlation between DH and nitrogen solubilization indicates that not all the solubilized proteins during digestion are actually hydrolyzed.

#### 3.3.3. Disappearance of intact protein

Disappearance of intact protein was monitored by reducing SDS-PAGE, as shown in Fig. 7. During gastric digestion, proteins were slightly digested, and large peptides around 10 kDa appeared on the gels. The low gastric disappearance of intact protein agrees with the low DH in the GP (Fig. 5). After 10 min in the IP, large peptides were cleaved into much smaller peptides. From I10 to I60, it is obvious in SP and PP samples that this cleavage into peptides further increased. However, for SP-G and PP-G, the peptides were not digested further, agreeing with the DH results that no significant increase in DH was found between I10 and I60 (Fig. 5).

Furthermore, the bands of the highly glycated proteins (T48) were faint, and almost only the digestive enzymes were visible on the gels. On the one hand, both SP-G and PP-G had the lowest starting solubility at T48, and they were more likely to be digested in the form of insoluble

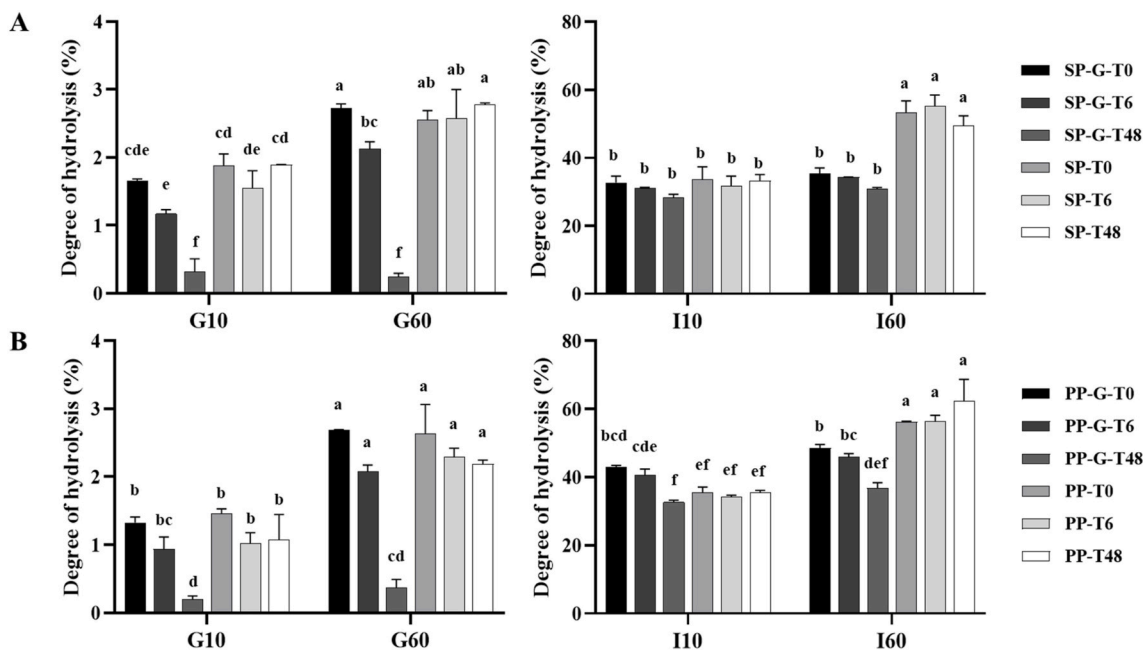


**Fig. 5.** Degree of hydrolysis of (A) SP-G and SP as well as (B) PP-G and PP upon different heating durations, after *in vitro* infant digestion. G10 and G60: samples after gastric digestion for 10 min and 60 min, respectively; and I10 and I60: samples after intestinal digestion for 10 min and 60 min, respectively. Error bars represent standard deviations of duplicates. Statistical differences were analyzed with ANOVA and Duncan post-hoc test. Different letters above the bars represent significant differences ( $p < 0.05$ ).

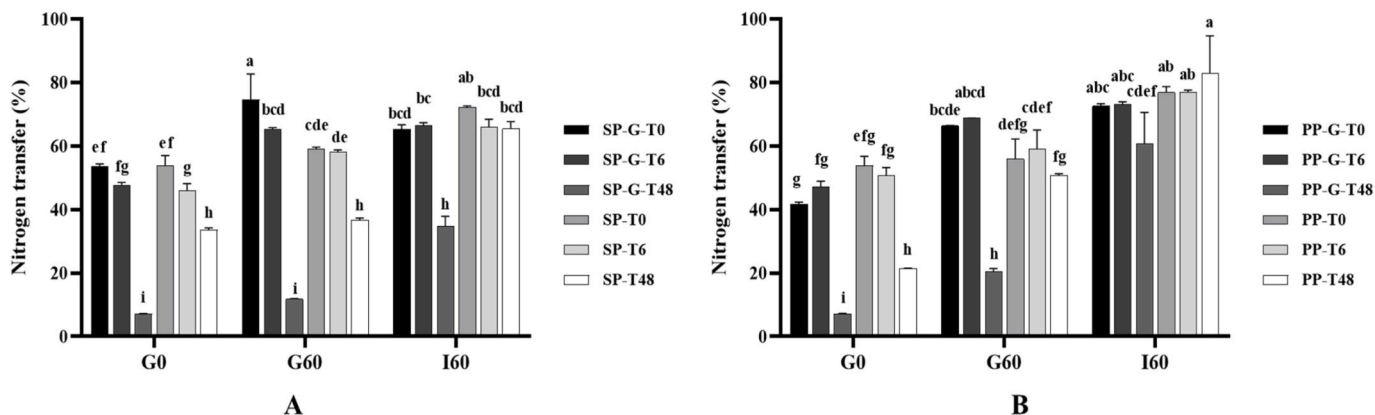


**Fig. 6.** Nitrogen transfer of (A) SP-G and SP as well as (B) PP-G and PP upon different heating durations, after *in vitro* infant digestion. G0: samples before digestion; G60: samples after gastric digestion for 60 min; and I60: samples after intestinal digestion for 60 min. Error bars represent standard deviations of digestion duplicates. Statistical differences were analyzed with ANOVA and Duncan post-hoc test. Different letters above the bars represent significant differences ( $p < 0.05$ ).

aggregates. During digestion, the formed peptides of low molecular weights went into the digestive fluids. On the other hand, samples were centrifuged to remove the insoluble parts, and only the supernatants were used for SDS-PAGE. Taken together, although the DH and the soluble nitrogen increased, the bands were still not visible on the gels, due to the absence of intact proteins in the supernatants.

### 3.4. Effect of dry heating and glycation on protein digestibility

To summarize, for glucose-containing SP-G and PP-G, longer dry heating contributed to a higher level of glycation, which was manifested by the decrease in lysine and the increase in furosine and CML (Fig. 1), as well as the enhanced browning (Table 1). The variation in the subunit composition of soluble proteins also confirmed this (Fig. 2). Furthermore, aggregation happened for all the glycated samples (Fig. 3); glycation lowered the surface hydrophobicity of soluble proteins, because of the formation of hydrophilic glycation products on the protein surface

(Fig. 4). Among all the samples, the highly-glycated samples at T48 had the largest aggregates as well as the lowest surface hydrophobicity.

However, for glucose-free SP and PP, no glycation occurred during dry heating (Fig. 1). Thus, the heating itself and not the glycation was the dominant driving force of the physicochemical changes. To be specific, the subunit composition and the surface hydrophobicity of soluble proteins remained unchanged after dry heating (Figs. 2 and 4). In addition, no soluble aggregates were found in the supernatants, but aggregation in the protein suspensions was seen (Fig. 3). It was noticed that dry heating contributed to a weaker aggregation when compared to heat-induced glycation, as confirmed by the PSD results and the reduced solubility (Figs. 3 and 6).

In terms of the overall digestibility, i.e., degree of hydrolysis and the disappearance of intact protein (Figs. 5 and 7), for glucose-free samples, no significant difference was found among different dry heating durations. Despite the increased aggregation during dry heating, these aggregates were mostly formed via non-covalent forces and therefore were

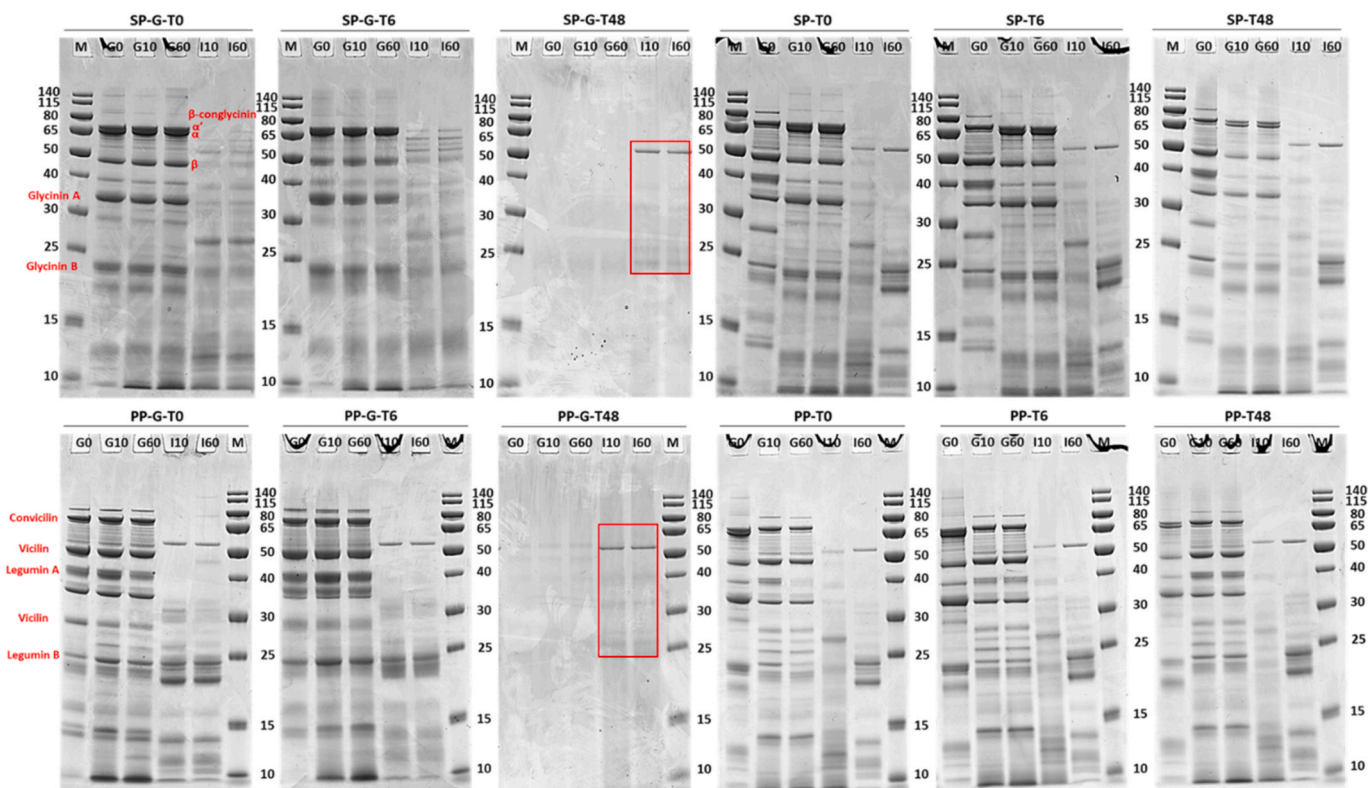


**Fig. 7.** Disappearance of intact protein of SP-G, PP-G, SP and PP upon different heating durations, after *in vitro* infant digestion. Lane G0: samples before digestion; lane G10 and G60: samples after gastric digestion for 10 min and 60 min, respectively; lane I10 and I60: samples after intestinal digestion for 10 min and 60 min, respectively; and lane M: molecular weight marker from 10 to 140 kDa. Solid boxes in red refer to the digestive enzymes from pancreatin. (For interpretation of the references to color in this figure legend, the reader is referred to the Web version of this article.)

easy to break down during digestion. Their accessibility to enzymes was thus not hindered. To conclude, the gastro-intestinal digestion was not affected for glucose-free samples.

As for SP-G and PP-G, the resistance to gastric digestion was apparent, especially in the samples at T48. It is known that pepsin preferentially cleaves at hydrophobic amino acid residues (Hall & Moraru, 2022). With enhanced glycation, the surface hydrophobicity of glucose-containing samples was decreased, while aggregation happened simultaneously (Figs. 3 and 4). It is possible that when dry heating is extended, the hydrophobic areas of proteins are buried inside, leading to reduced accessibility to pepsin. Furthermore, in terms of intestinal digestion, glycation nearly had nearly no impact on it. Only the DH of PP-G-T6 and PP-G-T48 significantly differed (Fig. 5). This can be explained by the use of pancreatin in this study. Although the tryptic cleavage sites might be blocked by glycation, other proteases and peptidases present in pancreatin, such as chymotrypsin, can still contribute to the protein digestion and compensate for the limited tryptic hydrolysis, being in line with the conclusion from Zenker et al. (2020). However, as discussed before, PP-G was more sensitive to dry heating, at T48, the glycation was more intense than SP-G (Fig. 1). Due to that, the tryptic digestion of PP-G was more inhibited, and such inhibition was not fully offset by other pancreatic enzymes, hence the significant decrease in the DH between T6 and T48. Therefore, it seems that the final intestinal digestion of glucose-containing samples was not affected. However, the different gastric digestion behavior of the glycated proteins may generate differences in peptides in the intestinal phase, and may therefore alter the form in which proteins are presented to the immune system, leading to different immunological responses.

#### 4. Conclusion

In the presence of glucose, dry heating at 60 °C led to the glycation

and aggregation of soy and pea proteins. These structural changes had a negative effect on gastric digestion, whereas the intestinal digestion was influenced to a much smaller extent. Moreover, for those proteins that were heated without glucose, longer dry heating only led to limited aggregation, but had no consequences for both gastric and intestinal digestion. Furthermore, future work should study the peptidomics of the intestinal digesta, to see the overall picture of peptides, as well as the immunoreactive peptides that may affect the immunological response. In addition, using *in vivo* studies to further confirm our findings might be interesting.

#### CRedit authorship contribution statement

**Jiaying Tang:** Conceptualization, Methodology, Formal analysis, Visualization, Software, Writing – original draft. **Harry J. Wichers:** Conceptualization, Supervision, Writing – review & editing. **Kasper A. Hettinga:** Conceptualization, Supervision, Software, Validation, Writing – review & editing, Funding acquisition.

#### Declaration of competing interest

The authors declare that they have no known competing financial interests or personal relationships that could have appeared to influence the work reported in this paper.

#### Data availability

Data will be made available on request.

#### Acknowledgment

This work was financially supported by the China Scholarship

Council (No.201906350087).

## References

- Charlton, A. J., Baxter, N. J., Khan, M. L., Moir, A. J. G., Haslam, E., Davies, A. P., et al. (2002). Polyphenol/peptide binding and precipitation. *Journal of Agricultural and Food Chemistry*, 50(6), 1593–1601. <https://doi.org/10.1021/jf010897z>
- Consoli, L., Dias, R. A. O., Rabelo, R. S., Furtado, G. F., Sussulini, A., Cunha, R. L., et al. (2018). Sodium caseinate-corn starch hydrolysates conjugates obtained through the Maillard reaction as stabilizing agents in resveratrol-loaded emulsions. *Food Hydrocolloids*, 84, 458–472. <https://doi.org/10.1016/j.foodhyd.2018.06.017>
- Corzo-Martínez, M., Soria, A. C., Belloque, J., Villamiel, M., & Moreno, F. J. (2010). Effect of glycation on the gastrointestinal digestibility and immunoreactivity of bovine  $\beta$ -lactoglobulin. *International Dairy Journal*, 20(11), 742–752. <https://doi.org/10.1016/j.idairyj.2010.04.002>
- European Commission. (2016). Commission Delegated Regulation (EU) 2016/127 of 25 September 2015 supplementing Regulation (EU) No 609/2013 of the European Parliament and of the Council as regards the specific compositional and information requirements for infant formula and follow-on formula and as regards requirements on information relating to infant and young child feeding (Text with EEA relevance). Retrieved from <https://eur-lex.europa.eu/legal-content/EN/TXT/PDF/?uri=CELEX:32016R0127&from=EN>.
- Feng, J., Berton-Carabin, C. C., Atac Mogol, B., Schroen, K., & Fogliano, V. (2021). Glycation of soy proteins leads to a range of fractions with various supramolecular assemblies and surface activities. *Food Chemistry*, 343, Article 128556. <https://doi.org/10.1016/j.foodchem.2020.128556>
- Fu, G., Xu, Z., Luo, C., Xu, L., Chen, Y., Guo, S., ... Wan, Y. (2021). Modification of soy protein isolate by Maillard reaction and its application in microencapsulation of *Limosilactobacillus reuteri*. *Journal of Bioscience and Bioengineering*, 132(4), 343–350. <https://doi.org/10.1016/j.jbiosc.2021.06.007>
- Gilani, G. S., Cockell, K. A., & Sepehr, E. (2019). Effects of antinutritional factors on protein digestibility and amino acid availability in foods. *Journal of AOAC International*, 88(3), 967–987. <https://doi.org/10.1093/jaoac/88.3.967>
- Gorissen, S. H. M., Crombag, J. J. R., Senden, J. M. G., Waterval, W. A. H., Bierau, J., Verdijk, L. B., et al. (2018). Protein content and amino acid composition of commercially available plant-based protein isolates. *Amino Acids*, 50(12), 1685–1695. <https://doi.org/10.1007/s00726-018-2640-5>
- Hall, A. E., & Moraru, C. I. (2022). Comparative effects of high pressure processing and heat treatment on in vitro digestibility of pea protein and starch. *Npj Science of Food*, 6(1), 2. <https://doi.org/10.1038/s41538-021-00116-0>
- Hemmler, D., Gonsior, M., Powers, L. C., Marshall, J. W., Rychlik, M., Taylor, A. J., et al. (2019). Simulated sunlight selectively modifies Maillard reaction products in a wide array of chemical reactions. *Chemistry - A European Journal*, 25(57), 13208–13217. <https://doi.org/10.1002/chem.201902804>
- Kavanagh, G. M., Clark, A. H., & Ross-Murphy, S. B. (2000). Heat-induced gelation of globular proteins: Part 3. Molecular studies on low pH  $\beta$ -lactoglobulin gels. *International Journal of Biological Macromolecules*, 28(1), 41–50. [https://doi.org/10.1016/S0141-8130\(00\)00144-6](https://doi.org/10.1016/S0141-8130(00)00144-6)
- Kutzli, L., Weiss, J., & Gibis, M. (2021). Glycation of plant proteins via Maillard reaction: Reaction chemistry, technofunctional properties, and potential food application. *Foods*, 10(2), 376. <https://doi.org/10.3390/foods10020376>
- Le Roux, L., Menard, O., Chacon, R., Dupont, D., Jeantet, R., Deglaire, A., et al. (2020). Are faba bean and pea proteins potential whey protein substitutes in infant formulas? An in vitro dynamic digestion approach. *Foods*, 9(3), 362. <https://doi.org/10.3390/foods9030362>
- Li, X., Huang, J., Wang, Z., Jiang, X., Yu, W., Zheng, Y., ... He, N. (2014). Alkaline extraction and acid precipitation of phenolic compounds from longan (*Dimocarpus longan* L.) seeds. *Separation and Purification Technology*, 124, 201–206. <https://doi.org/10.1016/j.seppur.2014.01.030>
- Li, X., Li, Y., Hua, Y., Qiu, A., Yang, C., & Cui, S. (2007). Effect of concentration, ionic strength and freeze-drying on the heat-induced aggregation of soy proteins. *Food Chemistry*, 104(4), 1410–1417. <https://doi.org/10.1016/j.foodchem.2007.02.003>
- Martín-Cabrejas, M. A., Aguilera, Y., Pedrosa, M. M., Cuadrado, C., Hernández, T., Díaz, S., et al. (2009). The impact of dehydration process on antinutrients and protein digestibility of some legume flours. *Food Chemistry*, 114(3), 1063–1068. <https://doi.org/10.1016/j.foodchem.2008.10.070>
- Ménard, O., Bourlieu, C., De Oliveira, S. C., Dellarosa, N., Laghi, L., Carrière, F., ... Deglaire, A. (2018). A first step towards a consensus static in vitro model for simulating full-term infant digestion. *Food Chemistry*, 240, 338–345. <https://doi.org/10.1016/j.foodchem.2017.07.145>
- Mulet-Cabero, A.-I., Rigby, N. M., Brodtkorb, A., & Mackie, A. R. (2017). Dairy food structures influence the rates of nutrient digestion through different in vitro gastric behaviour. *Food Hydrocolloids*, 67, 63–73. <https://doi.org/10.1016/j.foodhyd.2016.12.039>
- Muliterno, M. M., Rodrigues, D., de Lima, F. S., Ida, E. I., & Kurozawa, L. E. (2017). Conversion/degradation of isoflavones and color alterations during the drying of okara. *Lebensmittel-Wissenschaft & Technologie*, 75, 512–519. <https://doi.org/10.1016/j.lwt.2016.09.031>
- de Oliveira, F. C., Coimbra, J. S. d. R., de Oliveira, E. B., Zuñiga, A. D. G., & Rojas, E. E. G. (2016). Food protein-polysaccharide conjugates obtained via the maillard reaction: A review. *Critical Reviews in Food Science and Nutrition*, 56(7), 1108–1125. <https://doi.org/10.1080/10408398.2012.755669>
- Olsen, J. V., Ong, S.-E., & Mann, M. (2004). Trypsin cleaves exclusively c-terminal to arginine and lysine residues. *Molecular & Cellular Proteomics*, 3(6), 608–614. <https://doi.org/10.1074/mcp.T400003-MCP200>
- Rivera del Rio, A., Opazo-Navarrete, M., Cepero-Betancourt, Y., Tabilo-Munizaga, G., Boom, R. M., & Janssen, A. E. M. (2020). Heat-induced changes in microstructure of spray-dried plant protein isolates and its implications on in vitro gastric digestion. *Lebensmittel-Wissenschaft & Technologie*, 118, Article 108795. <https://doi.org/10.1016/j.lwt.2019.108795>
- Rutherford, S. M., Fanning, A. C., Miller, B. J., & Moughan, P. J. (2014). Protein digestibility-corrected amino acid scores and digestible indispensable amino acid scores differentially describe protein quality in growing male rats. *Journal of Nutrition*, 145(2), 372–379. <https://doi.org/10.3945/jn.114.195438>
- Schong, E., & Famelart, M.-H. (2017). Dry heating of whey proteins. *Food Research International*, 100, 31–44. <https://doi.org/10.1016/j.foodres.2017.08.057>
- Spotti, M. J., Loyeau, P. A., Marangon, A., Noir, H., Rubiolo, A. C., & Carrara, C. R. (2019). Influence of Maillard reaction extent on acid induced gels of whey proteins and dextrans. *Food Hydrocolloids*, 91, 224–231. <https://doi.org/10.1016/j.foodhyd.2019.01.020>
- Stewart, O. J., Raghavan, G. S. V., Orsat, V., & Golden, K. D. (2003). The effect of drying on unsaturated fatty acids and trypsin inhibitor activity in soybean. *Process Biochemistry*, 39(4), 483–489. [https://doi.org/10.1016/S0032-9592\(03\)00130-4](https://doi.org/10.1016/S0032-9592(03)00130-4)
- Tamanna, N., & Mahmood, N. (2015). Food processing and Maillard reaction products: Effect on human health and nutrition. *International journal of food science*. <https://doi.org/10.1155/2015/526762>, 2015, 526762-526762.
- Tang, J., Wichers, H. J., & Hettinga, K. A. (2022). Heat-induced unfolding facilitates plant protein digestibility during in vitro static infant digestion. *Food Chemistry*, 375, Article 131878. <https://doi.org/10.1016/j.foodchem.2021.131878>
- Troise, A. D., Fiore, A., Roviello, G., Monti, S. M., & Fogliano, V. (2015). Simultaneous quantification of amino acids and Amadori products in foods through ion-pairing liquid chromatography–high-resolution mass spectrometry. *Amino Acids*, 47(1), 111–124. <https://doi.org/10.1007/s00726-014-1845-5>
- Wada, Y., & Lönnnerdal, B. (2014). Effects of different industrial heating processes of milk on site-specific protein modifications and their relationship to in vitro and in vivo digestibility. *Journal of Agricultural and Food Chemistry*, 62(18), 4175–4185. <https://doi.org/10.1021/jf501617s>
- Wang, W., Yuan, P., Zhou, J., & Gu, Z. (2021). Effect of temperature and pH on the gelation, rheology, texture, and structural properties of whey protein and sugar gels based on Maillard reaction. *Journal of Food Science*, 86(4), 1228–1242. <https://doi.org/10.1111/1750-3841.15659>
- Xu, B. J., Yuan, S. H., & Chang, S. K. C. (2007). Comparative analyses of phenolic composition, antioxidant capacity, and color of cool season legumes and other selected food legumes. *Journal of Food Science*, 72(2), S167–S177. <https://doi.org/10.1111/j.1750-3841.2006.00261.x>
- Yuksel, Z., Avci, E., & Erdem, Y. K. (2010). Characterization of binding interactions between green tea flavanoids and milk proteins. *Food Chemistry*, 121(2), 450–456. <https://doi.org/10.1016/j.foodchem.2009.12.064>
- Zenker, H. E., Ewaz, A., Deng, Y., Savelkoul, H. F. J., van Neerven, R. J. J., De Jong, N. W., ... Teodorowicz, M. (2019). Differential effects of dry vs. wet heating of beta-lactoglobulin on formation of sRAGE binding ligands and sigE epitope recognition. *Nutrients*, 11(6). <https://doi.org/10.3390/nu11061432>
- Zenker, H. E., Raupbach, J., Boeren, S., Wichers, H. J., & Hettinga, K. A. (2020). The effect of low vs. high temperature dry heating on solubility and digestibility of cow's milk protein. *Food Hydrocolloids*, 109, Article 106098. <https://doi.org/10.1016/j.foodhyd.2020.106098>
- Zhao, S., Huang, Y., McClements, D. J., Liu, X., Wang, P., & Liu, F. (2022). Improving pea protein functionality by combining high-pressure homogenization with an ultrasound-assisted Maillard reaction. *Food Hydrocolloids*, 126, Article 107441. <https://doi.org/10.1016/j.foodhyd.2021.107441>